Hyperactive EGF receptor, Jaks and Stat3 signaling promote enhanced colony-forming ability, motility and migration of cisplatin-resistant ovarian cancer cells

Peibin Yue[1], **Xiaolei Zhang**[1], **David Paladino**[1], **Bhaswati Sengupta**[1], **Sarfraz Ahmad**[2], **Robert W. Holloway**[2], **Susan B. Ingersoll**[2], and **James Turkson**[1,*]

[1]Burnett School of Biomedical Sciences, University of Central Florida College of Medicine, 6900 Lake Nona Blvd, Orlando, FL 32827

[2]Florida Hospital Gynecologic Oncology, Florida Hospital Cancer Institute, 2501 N. Orange Ave., Suite 800, Orlando, FL 32804

Abstract

We present evidence that the cisplatin-resistant human ovarian cancer lines, A2780S/CP1 (S/CP1), A2780S/CP3 (S/CP3), and A2780S/CP5 (S/CP5), derived by subjecting the sensitive A2780S ovarian cancer line to multiple rounds of cisplatin treatments followed by recovery and are resistant to 1, 3, and 5 µM cisplatin, respectively, have increased colony-forming ability and altered morphology that is consistent with enhanced motility, migration, and invasiveness *in vitro*. The malignant phenotype progresses with increasing resistance and is associated with hyperactive epidermal growth factor receptor (EGFR)/extracellular signal-regulated kinase (Erk)1/2 and Janus kinases (Jaks), aberrant Signal Transducer and Activator of Transcription (Stat) 3 activation promoted by EGFR and Jaks, and epithelial-mesenchymal transition (EMT) *in vitro*. Survivin and FLIP anti-apoptotic factors, vascular endothelial growth factor (VEGF), and matrix metalloproteinase activities are also elevated in the resistant cells. Accordingly, the ectopic expression of constitutively-active Stat3C in the sensitive A2780S cells diminished cisplatin sensitivity. The inhibition of EGFR or Stat3 activity repressed Survivin, VEGF and Vimentin expression and the colony-forming potential, viability, motility, and migration of the resistant cells, and sensitized them to cisplatin. Analysis of human ovarian cancer patients' tumor tissues shows aberrantly-active EGFR and Stat3 that in certain cases correlate with Vimentin over-expression. Intra-peritoneal mouse xenograft studies revealed, compared to the sensitive A2780S line that had low tumor incidence restricted to the ovary, a high tumor incidence for the resistant S/CP3 and S/CP5 lines that formed tumor nodules at several locations on the small-intestine and colon, and which responded poorly to cisplatin, but were sensitive to concurrent treatment with cisplatin and EGFR or Stat3 inhibitor. Hyperactive EGFR signaling through Stat3 and the Jak-Stat3 activity together promote ovarian cancer progression to cisplatin resistance and therefore represent targets for preventing the development of cisplatin resistance and the recurrent disease during cisplatin therapy in ovarian cancer.

*Address correspondence to: James Turkson, Burnett School of Biomedical Sciences, University of Central Florida College of Medicine, 6900 Lake Nona Blvd, Orlando, FL 32827, Tel. 407-266-7031, james.turkson@ucf.edu.
New address: Cancer Biology & Experimental Therapeutics Programs, University of Hawai'i Cancer Center, University of Hawai'i at Manoa, Biomedical Sciences Building, Suite 222J, 651 ILALO Street, Honolulu, Hawai'i 96813-5525, Tel. 808-356-5784, jturkson@cc.hawaii.edu

Conflict of interest

The authors declare no conflict of interest.

Keywords

Cisplatin-resistance; ovarian cancer; EGF receptor; Stat3; Jaks; motility; migration

Introduction

A common feature of ovarian cancer is the wide dissemination in the peritoneum at the time of clinical presentation, which presents challenges to therapy on how to eradicate the disease tissue. cisplatin and related compounds are widely used for treating ovarian cancer. However, recurrent and resistant disease develop in a large percentage of the treated patients (Brabec and Kasparkova, 2005; Kelland *et al.*, 1999; Gonzalez *et al.*, 2001). Several events have been suggested to be involved in the development of resistance to cisplatin and related compounds, including reduced drug transport and DNA platination, increased nucleotide excision repair and loss of mismatch repair, and increased tolerance of DNA adducts (Brabec and Kasparkova, 2005; Kelland *et al.*, 1999). However, the molecular mechanisms for the resistant phenotype remains poorly defined.

Studies in the last few decades have led to the understanding that cancer is fundamentally a disease of molecular aberrations (Blume-Jensen and Hunter, 2001). Hyperactivation of the EGFR pathway is implicated in many human cancers (Blume-Jensen and Hunter, 2001; Chan *et al.*, 2005; Dancey and Freidlin, 2003). Moreover, the Stat3 protein, a member of the STAT family of latent cytoplasmic transcription factors, which are linked to and are phosphorylated by EGFR and other tyrosine kinases, such as Jaks is aberrantly activated with a high frequency in ovarian and many other human tumors (Burke *et al.*, 2001; Huang *et al.*, 2000). Of significance is the accumulation of anti-apoptotic events, such as Bcl-2, Bcl-xL, and PI 3-kinase/Akt activity in the recurrent and resistant ovarian cancer (Brabec and Kasparkova, 2005; Richardson and Kaye, 2005), granted that constitutively-active Stat3-mediated dysregulation of gene expression is a well recognized mechanism to promote malignant tumorigenesis, and tumor progression (see (Bowman *et al.*, 2000; Darnell, 2005; Turkson, 2004; Yu and Jove, 2004) for reviews). Accordingly, emerging evidence associates hyperactive EGFR and Jak-Stat3 pathways with drug resistance through the induction of anti-apoptotic factors, including Bcl-2, Bcl-xL, Survivin and XIAP (Aoki *et al.*, 2003; Bhattacharya *et al.*, 2005; Catlett-Falcone *et al.*, 1999; Gritsko *et al.*, 2006; Kassouf *et al.*, 2005; Richardson and Kaye, 2005). However, the roles of EGFR and Stat3 in cisplatin resistance have remained poorly understood. Novel insights into the mechanistic pathways that promote cisplatin resistance in ovarian cancer will provide new and effective treatment modalities for this disease.

Using *in vitro* cisplatin resistant models developed by repeated sequential treatments followed by rest periods, we present evidence of enhanced colony-forming ability, motility, migration, and invasiveness of the cisplatin-resistant ovarian cancer cells. These changes are associated with Survivin, FLIP, and VEGF overexpression, increased matrix metalloproteinase activities, and the induction of epithelial-mesenchymal transition (EMT) *in vitro*, all of which are sensitive to inhibition of hyperactive EGFR, Jaks or Stat3. The resistant ovarian cancer cells also showed increased tumorigenicity and dissemination in the peritoneal area *in vivo*, with tumor nodules that were insensitve to cisplatin, but responded to a combined cisplatin treatment with the inhibition of hyperactive EGFR or Stat3 activity. Present study indicates hyperactive EGFR, largely through Stat3 activity and the Jak-Stat3 activity contribute to promoting the cisplatin-resistant phenotype.

Results

Cisplatin-resistant ovarian cancer cells show slower proliferation, enhanced colony-forming potential, and increased motility, migratory and invasive properties *in vitro*

The cisplatin-sensitive human ovarian cancer line, A2780S was subjected to repeated sequential treatments, with drug-free recovery time, over a period of 2–6 months to derive A2780S/CP1 (S/CP1), A2780S/CP3 (S/CP3) and A2780S/CP5 (S/CP5), which resistant to 1, 3 or 5 μM cisplatin, respectively, and show weak sensitivity to cisplatin in viability assays (Fig. 1A), with IC_{50} values of 3, 4.2 and 4.7 μM, respectively, compared to A2780S cells, with IC_{50} of 0.6 μM (Fig. 1A, insert). Trypan blue exclusion/phase-contrast microscopy for viable cells confirmed the high cisplatin-sensitivity of A2780S (Fig. 1B, top left panel), and the decreasing sensitivity of S/CP1, S/CP3 and S/CP5 (Fig. 1B, compare cisplatin to control), and also show the resistant cells are slower proliferating, compared to A2780S cells (Fig. 1C). By contrast, the resistant S/CP3 and S/CP5 showed similar sensitivity as the sensitive A2780S line to paclitaxel (Supplemental Fig. S1), suggesting the altered phenotype could be restricted to cisplatin. Colony survival assays show larger colony numbers and sizes for the resistant cells that progressed with increasing resistance, compared to the sensitive A2780S cells (Fig. 1D, Control, Con), and a similar trend in colony numbers were observed when the resistant lines, S/CP1, S/CP3 and S/CP5 were treated once with 1, 3, and 5 μM cisplatin, compared to A2780S cells treated once with 1 μM cisplatin, as observed in photomicrographs (Fig. 1D(i), cisplatin) or in the enumerated colony numbers (Fig. 1D(ii), cisplatin).

Altered morphology that progressed with increasing resistance is evident under phase-contrast microscopy (Fig. 1E, compared S/CP1, S/CP3 and S/CP5 to A2780S) and suggested increased motility and/or migratory properties. Results from wound-healing assays over 24–72 h period, and presented as either photomicrographs (Fig. 1F(i)) or distance traveled by the cell front into the denuded (motility) (Fig. 1F(ii)) showed the resistant lines, S/CP3 and S/CP5 exhibit increased motility with increasing degree of cisplatin resistance (Fig. 1F). *In vitro* Bio-Coat migration chamber assay similarly showed higher number of migrated S/CP3 and S/CP5 lines over a 22 h period, compared to A2780S cells (Fig. 1G). Consistent with the observed morphological features that suggest enhanced metastatic potential, as is evident in cisplatin resistance in ovarian cancer and in tumor progression (Bowden *et al.*, 1999; Desai *et al.*, 2008), gelatin zymography assay to assess the matrix proteolytic activity of the conditioned media (Matsuo *et al.*, 2007) showed more intense bands indicative of high gelatinolytic activity, and hence increased matrix metalloproteinases (MMP) activity for media from 48-h or 72-h cultures of the resistant lines S/CP3 and S/CP 5 (Fig. 1H). The S/CP5 cell-culture media showed the strongest MMP-2 and MMP-9 activities that increased over 48–72 h (Fig. 1H). For the moderately resistant S/CP3 line, a higher MMP-9 activity was associated with the 72-h culture, with little change in the MMP-2 activity, compared to the cultures of A2780 cells (Fig. 1H).

Enhanced EGFR, Jaks and Stat3 activation in cisplatin-resistant ovarian cancer lines

We next explored the suggested role of EGFR and Jaks in ovarian cancer and cisplatin resistance (Selvendiran *et al.*, 2008; Song *et al.*, 2004). Immunoblotting analysis showed high pY1173EGFR and pY1068EGFR levels, moderate pY1086EGFR levels, high pJak2 levels, and elevated pErk1/2 levels in all three resistant cells, while pAkt levels remained unchanged (Fig. 2A). By contrast, pY416Src levels were significantly reduced in the resistant lines, in parallel with diminished pY845EGFR levels, a known Src phosphorylation site on EGFR (Tice *et al.*, 1999), suggesting Src activity does not contribute to EGFR activation in cisplatin resistance, and a decreased pFAK levels (Fig. 2A), consistent with the diminished Src activity. Total EGFR, Src, Jak2, Erk1/2, Akt and FAK protein levels

remained unchanged. Given the increased pY1068EGFR levels (Fig. 2A), which is a Stat3-binding site (Shao *et al.*, 2003), we evaluated Stat3 activation status. Immunoblotting analysis show that both pY705Stat3 and pS727Stat3 levels are elevated in all three resistant cells, while total Stat3 protein remained unchanged (Fig. 2A). Overall, the extent of EGFR, Jaks and Stat3 activation did not necessarily correlate with the degree of cisplatin resistance. In particular, pY1173EGFR, pJak2, pS727Stat3, and pErk1/2 were highest in the most resistant S/CP5 line (Fig. 2A), pY1068EGFR and pY705Stat3 were highest in S/CP1 and S/CP3 cells (Fig. 2A), while pY1086EGFR was only moderately elevated in all three resistant lines. These differences further underscore the variability in the molecular changes in the resistant phenotype and suggest heterogeneity of the cells that make up the resistant tumor.

Immunoblotting analysis further show that treatment with the selective EGFR inhibitor, ZD1839 (ZD) suppresses phospho-EGFR levels to background (Fig. 2B), which occurs in parallel with reduced pErk1/2, pY705Stat3 and pS727Stat3 in S/CP3 and S/CP5 cells (Fig. 2B), indicating hyperactive EGFR promotes aberrant phosphorylation of Erk1/2, S727Stat3 and Y705Stat3 in cisplatin-resistant ovarian cancer cells. The total proteins remained unchanged. These findings were validated by siRNA kockdown of EGFR in S/CP3 and S/CP5, which decreased pErk1/2, and pY705Stat3, and pS727Stat3 levels (Fig. 2C), while the total Erk1/2 and Stat3 proteins remained unchanged. To determine if Erk1/2 activity mediates the phosphorylation of S727Stat3, the resistant lines were treated with the MAPK kinase (MEK) inhibitor, PD98059 (PD), which decreased pErk1/2 and pS727Stat3 levels in PD-treated S/CP3 and S/CP5 cells (Fig. 2D), indicating Erk1/2 phosphorylates S727Stat3. Immunoblotting analysis also showed moderate suppression of constitutive pY705Stat3, but not pS727Stat3 levels in resistant cells treated with the Jak inhibitor, AG490 (Fig. 2E), suggesting Jak activities contribute to, but are not the predominant mediators of aberrant Stat3 activation in cisplatin resistance.

Hyperactive EGFR, Jaks and Stat3 promote enhanced colony-forming, motility, and migration properties of cisplatin resistant ovarian cancer cells *in vitro*

We were interested in investigating further the molecular underpinnings of the enhanced colony-forming ability, motility and migration and the role of hyperactive EGFR, Erk1/2, Stat3 and Jak kinase. Results from colony survival assays of S/CP3 and S/CP5 presented as photomicrographs (Fig. 3A(i)) or number of colonies (Fig. 3A(ii)) show that inhibition of MEK-Erk1/2 strongly diminished the colony sizes (Fig. 3A), but only moderately reduced the colony numbers (Fig. 3A, PD, compared to control, Con), suggesting that the MEK-Erk1/2 arm of the EGFR pathway supports proliferation, but is not essential for the viability of the resistant cells. By contrast, the inhibition of EGFR by ZD, or of Stat3 by S3I-201 (Siddiquee *et al.*, 2007b; Zhang *et al.*, 2010) strongly diminished both colony sizes and numbers (Fig. 3A, ZD, S3I-201), while the inhibition of Jaks by AG490 completely blocked colony formation (Fig. 3A, AG490). The observation that the inhibition of Stat3 activation alone reduced, but did not completely block colony formation suggests non-Stat3-dependent mechanisms contribute to the AG490-mediated complete block of colony formation. Altogether, our data indicate the MEK-Erk1/2 arm of EGFR signaling predominantly promotes the proliferation of the resistant cells, while the EGFR signaling through Stat3 activation and Jak-Stat3 signaling support proliferation and viability, thereby promoting the enhanced colony forming potential of the resistant cells. These findings are in contrast to the previous report that Stat3 activity is nonessential in the context of acquired chemoresistance (Villedieu *et al.*, 2006). Viability assay further showed a shift to the left of the cisplatin dose-response curves by co-treatment with ZD1839 or by S3I-201 (Fig. 3B, ZD and S3I), while the co-treatment with PD98059 only moderately shifted the dose-response curve to the left (Fig. 3B, PD), These findings strongly suggest the inhibition of EGFR or Stat3 activity substantially sensitized the resistant S/CP3 and S/CP5 cells to cisplatin, while the inhibition

of the MEK-Erk1/2 arm of the EGFR pathway only moderately sensitized the cells. Furthermore, A2780S/Stat3C line that ectopically expresses the artificially-designed, constitutively-active Stat3C showed poor sensitivity to cisplatin, with IC_{50} value of 3.5 µM (Supplemental Fig. S2, Stat3C), compared to sensitive parental A2780S cells, with IC_{50} value of 0.85 M for effect of cisplatin (Supplemental Fig. S2, Mock-transfected).

Results from wound-healing assay presented as photomicrographs (Fig. 3C(i)) or as the measured distance traveled by the cell front into the denuded area (motility) (Fig. 3C(ii)) show the inhibition of EGFR by ZD, or of Stat3 activity by S3I-201, or of Jak activity by AG490 diminished the motility of the resistant cells, with the inhibition of EGFR resulting in the strongest effect (Fig. 3C, ZD, S3I-201, and AG490, compared to DMSO). Similarly, *in vitro* Bio-Coat migration chamber assay showed that the treatment with the ZD, S3I-201, or AG490 diminished the numbers of migrated S/CP3 and S/CP5 cells (Fig. 3D, ZD, S3I-201, and AG490, compared to DMSO). The observation that the EGFR inhibition by ZD shows the strongest effect may be due to the inhibition of the EGFR-MEK-Erk1/2 and the EGFR-Stat3 pathways. Accordingly, the inhibition of the MEK-Erk1/2 by PD98059 (PD) had more effect on the motility and migration of S/CP5 cell, but not of S/CP3 cells (Fig. 3C and 3D, PD), suggesting that the MEK-Erk1/2 arm contributes to, but is not the predominant pathway that promotes the migration and motility of cisplatin-resistant ovarian cancer cells.

Reciprocal expression E-Cadherin and Vimentin and the upregulation of F-actin and Cortactin in cisplatin-resistant ovarian cancer cells *in vitro* and in tumor tissues

We sought to investigate further the underlying molecular changes for the altered morphology and other phenotypic features. Immunoblotting analysis showed increased expression of F-actin, Cortactin, and phospho-Cortactin in the resistant lines, and a parallel decrease in paxillin expression, compared to the cisplatin-sensitive A2780S cells (Fig. 4A(i), left panel). ImageQuant analysis of the expression levels relative to β-actin are shown in Fig. 4A(i), right panel). Immunostaining with laser-scanning confocal microscopy imaging confirmed the higher F-actin expression and also showed its localization predominantly to the cellular protrusions (Fig. 4A(ii), white arrows). Moreover, the inhibition of EGFR, but not of Stat3 activation suppressed Cortactin expression (Fig. 4C, Cortactin), while neither EGFR nor Stat3 inhibition had any effect on F-actin expression or distribution (Fig. 4A(iii), and 4C, F-actin).

Reports show that the acquisition of the invasive behavior of ovarian cancer cells and the disease progression are associated with epithelial-to-mesenchymal transition (EMT), a process characterized by the upregulation of mesenchymal markers and the concomitant loss of epithelial markers, and altered cellular morphology (Ahmed *et al.*, 2007; Thiery, 2002). Thus, we sought to explore the relationship of the observed altered morphology and EMT. Immunoblotting analysis showed decreased E-Cadherin expression, accompanied by a parallel increased Vimentin expression that occurred in a progressive manner with increasing resistance (Fig. 4B(i)). Furthermore, the EMT regulatory transcription factor, Snail is upregulated in the most resistant, S/CP5, but not S/CP3 cells (Fig. 4B(ii)). Numbers in parenthesis are the expression levels of the respective proteiins relative to β-actin, as determined by ImageQuant are shown in parenthesis. Altogether, these events are consistent with the occurrence of EMT during the stages of the development of cisplatin resistance, consistent with reports that EMT contributes to drug resistance (Arumugam *et al.*, 2009; Lee *et al.*, 2008). Immunoblotting analysis further showed that the inhibition of EGFR by ZD or Stat3 by S3I-201 reduced Vimentin levels in S/CP3 and S/CP5 cells (Fig. 4C, Vimentin), and in the S/CP5 cells where Snail is over-expressed, the treatments with ZD or S3I-201 also suppressed Snail expression (Fig. 4C, Snail). Our data together show that hyperactive EGFR signaling that occurs in part through Stat3 promotes EMT during cisplatin resistance

development. These findings the parallel previous reports that associate EGFR and Stat3 activities with EMT in prostate and cervical cancers (Gan *et al.*, 2010; Lee *et al.*, 2008).

To provide clinical relevance, immunoblotting analysis of tissue lysates prepared from patients' tumor tissues was performed. Results show variable expressions of E-cadherin, Vimentin, and Snail, and differential activation of Stat3 (pTyr705Stat3) and of the Stat3-binding site, pY1068EGFR in the seven tumor tissues studied, S1, S2, S4, S8, S9, S10, and S11 (Fig. 5(i)). Specifically, Stat3 was activated in five of seven tissues, while EGFR was hyperactivated in four of seven tissues. Given that Stat3 or EGFR is inactive under basal conditions, that aberrant activation in four or five of the seven ovarian cancer tissues supports a role of hyperactive EGFR and Stat3 in ovarian cancer progression. ImageQuant analysis of each band of the immunoblots, reported as fold increase relative to β-Actin levels (Fig. 5(ii)), showed concurrent activation of (pTyr705)Stat3 and high Vimentin levels in two (S2 and S11) of seven tissues, and concurrently decreased pTyr705Stat3 and increased E-cadherin levels in two (S4 and S9) of seven tissues, indicating that in four out of seven ovarian cancer cases, aberrant Stat3 activation correlates with Vimentin over-expression or E-cadherin down-regulation. Hyperactive EGFR and Stat3 signaling, increased Vimentin expression, together with a decreased E-cadherin expression occurred in one (S11) of seven patients' tissues (Fig. 5(ii)). Snail expression was high in one (S10) of seven tissues, moderate in three (S1, S4, and S9) of seven tissues and low in the remaining three tissues (Fig. 5(i)); however, those levels did not show any correlation with the upregulated Vimentin or the aberrant Stat3 activation. On the clinical response to therapy, all of the seven patients responded. Per the clinical definition that clinical resistance is relapse within 6 months and sensitive is relapse after 12 months off therapy, differences in sensitivity were observed between the patients. The clinical drug responsiveness for six of the seven patients appeared to be partly or mainly consistent with the profile of pYStat3, Vimentin and/or pEGFR, while inconsistent for one patient. Also clearly, when pYStat3 and Vimentin were low, patients appeared to be clinically responsive to platin agents. Thus, the patients #S4, #S9 and #S10 were all responsive to platin agents, with low drug resistance (Fig. 5C), which would be consistent with the near low or low pYStat3 and Vimentin in the tumor tissues (Fig. 5A). Patient #S8 showed an extreme drug resistance, and patients #2 and #11 showed intermediate drug responsiveness (Fig. 5C), all of which are partly consistent with the moderate to high pYStat3 and Vimentin, with or without elevated pEGFR (Fig. 5A). By contrast, patient #S1 showed responsiveness to cisplatin and low drug resistance (Fig. 5C), which would be inconsistent with the moderate to high pYStat3, Vimentin, and pEGFR. We note however, that while patient #S1 showed platinum response to completed platinum-based therapy (for at least 9 months), the disease recurred 10 months post completion of platinum-based therapy. These results together show that aberrant EGFR and Stat3 activation occur in human ovarian tumor tissues, which correlate with the upregulation of Vimentin expression in certain ovarian cancer cases, and the elevated pYStat3 and Vimentin, with or without pEGFR is associated with altered clinical drug responsiveness in certain ovarian cancer cases.

Cisplatin resistance in ovarian cancer cells is associated with the upregulation of c-Myc, Survivin, FLIP, and VEGF

For further insight into the underlying molecular mechanisms of cisplatin resistance and the role of EGFR-Erk and Stat3 activation, we investigated known regulated genes and anti-apoptotic factors. Increased expression of c-Myc, Survivin and FLIP anti-apoptotic factors, and of VEGF were detected in the three resistant lines, S/CP1, S/CP3 and S/CP5 (Fig. 6A), consistent with the reports that associate anti-apoptotic factors with drug resistance (Gonzalez *et al.*, 2001; Ikuta *et al.*, 2005; Wang *et al.*, 2004). Interestingly, p53 levels were elevated, as previously reported (Fajac *et al.*, 1996), in parallel with decreased p21$^{WAF1/CIP1}$

expression (Fig. 6A). The elevated p53 protein in the resistant lines may be non-functional (Gallagher *et al.*, 1997), consistent with the report that non-functional p53 contributes to cisplatin resistance development (Gallagher *et al.*, 1997). Immunoblotting analysis further shows that the inhibition of hyperactive EGFR suppressed VEGF and Survivin expression in the resistant lines S/CP3 and S/CP5 (Fig. 6B), indicating that hyperactive EGFR signaling pathway promotes Survivin and VEGF induction in cisplatin resistance in ovarian cancer.

Increased tumorigenicity of cisplatin-resistant lines

Ovarian cancer disseminates widely in the peritoneal area at the time of presentation, and the recurrent disease is also frequently resistant to therapy. Given their high colony-forming ability and the enhanced motility and migratory properties *in vitro*, the cisplatin-resistant lines were used to develop *in vivo* models to further study the resistant phenotype and to characterize the tumor-forming and metastatic potential *in vivo*. Mice were inoculated with the sensitive and the resistant cells in the peritoneal area and monitored daily for 25–39 days post inoculation. After 25 days, animals were subjected to detailed examination. Consistent with their high colony-forming potential, 100% tumor incidence was observed for the most resistant line S/CP5, and 60% tumor incidence each for the moderately resistant, S/CP3 line and the sensitive line, A2780S (Fig. 7A, lower panel numbers). Significantly, mice inoculated with the more resistant S/CP5 cells, and to a lower extent, S/CP3 cells had more tumor nodules, compared to the sensitive A2780S line (Fig. 7A, S/CP5, arrows denote tumor nodules, and 7B), which were localized on the small-intestine and the colon (Fig. 7A, S/CP5). However, mice inoculated with the sensitive line, A2780S developed large tumors restricted to the ovary (Fig. 7A, A2780S, arrows, and Supplementary Fig. S3A, black arrow). Thus, the most resistant line, S/CP5 has an increased potential to form tumors and disseminate throughout the peritoneal area, compared to the sensitive A2780S cells. Histological analysis of the normal and tumor tissues are shown in Supplemental Fig. S3B) and reveals increased vascularization of the A2780S-derived ovarian tumor. Consistent with the *in vitro* data, mouse tumor xenografts established from the resistant S/CP5 line were insensitive to cisplatin treatment (Fig. 7C, Cis compared to untreated control, Con). Of therapeutic significance, co-treatment with the EGFR inhibitor, ZD1839 or the Stat3 inhibitor, S3I-201 sensitized the S/CP5 tumors to cisplatin-induced inhibition (Fig. 7C, Cis + ZD, and Cis + S3I-201).

Discussion

There is little understanding of the underlying mechanisms for the drug resistance of the recurrent disease. The present study demonstrates that cisplatin-resistant ovarian cancer cells possess an enhanced colony-forming potential and a dramatically altered morphology, consistent with increased motility, migration and invasiveness. These altered properties promote an increased tumor incidence and metastatic spread in the peritoneal area *in vivo*, as evidenced by the greater number of tumor nodules *in vivo* of the most resistant line, S/CP5 line, which are located on the colon and the small intestines, compared to the limited intra-peritoneal spread of the sensitive A2780S ovarian cancer line. These findings have important clinical implications and raise the possibility that the extensive intra-peritoneal spread of ovarian cancer in the patient at the time of diagnosis is reflective of a disease that is already progressed to the drug resistant stage, at which time the tumor cells possess molecular, morphological and cellular features as identified in the present study.

Reduced cell-cell interactions and dynamic cell–matrix adhesions contribute to increased motility and migratory behaviors reflective of the high metastatic spread that is common with recurrent ovarian cancer. As suggested by our studies, reduction in the activities of Src and its downstream target, FAK, which are important mediators of epithelial cell-cell interaction in non-migratory cells (Avizienyte and Frame, 2005), and increased Cortactin

and F-actin expression, and F-actin localization to the cellular extensions would all contribute to the high motility and migratory properties of the resistant cells. Furthermore, the increased Vimentin expression with the parallel decreased E-cadherin levels in cisplatin-resistant lines indicate that EMT process is a contributing factor to the progression to the metastatic spread (Lee *et al.*, 2008) and to the cisplatin-resistant phenotype (Arumugam *et al.*, 2009), as has been previously suggested. Evidently, hyperactive EGFR and the Jak-Stat3 pathways are key mediators of the altered phenotype and the EMT process that is associated with cisplatin resistance (Fig. 8). Specifically, aberrantly-active Stat3 promoted by hyperactive EGFR and Jaks and the EGFR-mediated Erk activity support the altered proliferation of the resistant cells. Contrary to our study and a previous report (Cui *et al.*, 2000) that implicate Erk activity in cisplatin resistance, it is reported that Erk activation is important in the response of renal epithelial or mouse proximal tubule cells to cisplatin (Arany *et al.*, 2004; Kim *et al.*, 2005), and that the loss of Erk activity may promote cisplatin-resistance (Villedieu *et al.*, 2006). Thus, the role of Erk in the cellular response or the lack thereof to cisplatin may be cell-type and context dependent. Additionally, our studies demonstrate that the enhanced colony-forming, motility and the migration properties of the resistant cells are largely dependent on hyperactive EGFR- and Jak-mediated aberrant Stat3 activation, with a minimal role for Erk activity (Fig. 8).

Aberrantly-active Stat3 has the propensity to promote drug resistance, as supported by our study and others (Burke *et al.*, 2001; Duan *et al.*, 2006; Selvendiran *et al.*, 2009). The incidence of constitutive Stat3 activation with the onset of cisplatin resistance *in vitro* for ovarian cancer cells that were originally cisplatin-sensitive and that showed no evidence of constitutively-active Stat3 suggests that the abnormal Stat3 activity may be one of the early events during the acquired resistance. This inference will be consistent with the ability of constitutive Stat3 activity to dysregulate anti-apoptotic and other tumor-supporting factors, such as Bcl-2, Mcl-1, and Bcl-xL (Bhattacharya *et al.*, 2005; Catlett-Falcone *et al.*, 1999; Epling-Burnette *et al.*, 2001; Huang *et al.*, 2000), Survivin (Aoki *et al.*, 2003; Gritsko *et al.*, 2006), and FLIP, and VEGF pro-angiogenic factor (Niu *et al.*, 2002) that support tumor cell survival, as present study show. Thus, the inhibition of hyperactive EGFR or Jak-Stat3 activity suppressed the expression of these factors and modulated the resistant phenotype *in vitro*. More importantly and of clinical and therapeutic significance, our studies establish that inhibitors of EGFR or Stat3 could be used in combination with cisplatin to prevent resistance and to sensitize resistant ovarian tumors to cisplatin. Altogether, the present study provides evidence that hyperactive EGFR and Jak-Stat3 signaling promote enhanced colony-forming, motility, and migratory properties and induce EMT as underlying mechanisms of cisplatin-resistance, changes that lead to increased tumorigenicity *in vivo* and metastatic spread in the peritoneal area of cisplatin-resistant ovarian cancers.

Materials and Methods

Cells and Reagents

The human ovarian cancer cells, A2780S were a kind gift from Dr. Jin Q. Cheng (Moffitt Cancer Center and Research Institute). The A2780S and the resistant cells, S/CP1, S/CP3 and S/CP5 were grown in Dulbecco's modified Eagle's medium/F12 (DMEM/F12) containing 10% heat-inactivated fetal bovine serum and 100 units/ml of penicillin/streptomycin (Pen/Strep). Stat3C construct has been previously reported (Bromberg *et al* 1999). All of the primary antibodies used were obtained from Cell Signaling Technology (Danvers, MA), except anti-VEGF antibody (Santa Cruz Biotech, Santa Cruz, CA) and antibody against F-actin from Abcam (Cambridge, MA).

Whole-cell lysate preparation and SDS-PAGE/Western Blot Analysis

Lysate preparation and immunoblotting analysis were performed as previously described (Turkson *et al.*, 1998; Zhang *et al.*, 2000).

Small-interfering RNA (siRNA) Transfection

EGFR siRNA were ordered from Dharmacon RNAi Technologies, Thermo Scientific (Lafayette, CO). Sequences used are: EGFR sense strand, 5′-GAAGGAAACUGAAUUCAAAUU-3′; EGFR antisense strand, 5′-pUUUGAAUUCAGUUUCCUUCUU-3′; control siRNA sense strand, 5′-AGUAAUACAACGGUAAAGAUU-3′; and control siRNA antisense strand, 5′-pUCUUUACCGUUGUAUUACUUU-3′. Transfection into cells was performed using 20 nM of siRNA and 8 μl Lipofectamine RNAiMAX (Invitrogen Corporation, Carlsbad, CA) in OPTI-MEM culture medium (Invitrogen).

Immunostaining with Laser-Scanning Confocal Imaging

Cells were grown on glass cover slips in multi-well plates. Cells were fixed with ice-cold methanol for 15 min, washed 3 times with 1X phosphate buffered saline (PBS), permeabilized with 0.2% Triton X-100 for 10 min, and further washed 3–4 times with PBS. Specimens were then blocked in 1% bovine serum albumin (BSA) for 30 min and incubated with anti-F-actin (Abcam) antibody at 1:50 dilution at 4 °C overnight. Subsequently, cells were rinsed 3 times with PBS, and incubated with Alexa fluor 546 mouse antibody (Invitrogen) for 1 h at room temperature in the dark. Specimens were then washed 3 times with PBS, mounted on slides with VECTASHIELD mounting medium (Vector Lab, Inc., Burlingame, CA), and examined immediately under a Leica TCS SP5 confocal microscope (Germany). Images were captured and processed using the Leica TCS SP 5 software.

Cell Proliferation/Viability Assay

Proliferating cells in 6-well or 96-well plates were untreated or treated once with cisplatin, 0–20 μM for 48 h or single concentration of cisplatin for up to 96 h, with or without treatment with ZD 1839 (5 μM), S3I-201 (50 μM), or PD98050 (20 μM) for 48 h, or treated with increasing concentrations of paclitaxel for 48 h. Viable cells were counted by trypan blue exclusion/phase contrast microscopy or assessed by CyQuant cell viability assay (Zhang *et al.*, 2010), according to manufacturer's (Invitrogen) instructions.

Transient Transfection of Cells and Treatment with Compound

Eighteen hours after seeding, cells were transiently-transfected with the Stat3C plasmids or mock-transfected. Twelve hours after transfection, cells were untreated (0.05% DMSO) or treated with cisplatin (0–20 μM) for an additional 48 h and subjected to CyQuant viability assay.

Colony Survival Assay

Studies were performed as previously reported (Zhang *et al.*, 2010). On the next day following seeding, cells were untreated or treated once with cisplatin or inhibitors and allowed to culture for 10–14 days until large colonies were visible. Colonies were fixed with methanol and stained with crystal violet (ThermoFisher, Pittsburgh, PA) for 2 h, and the number of colonies was counted or photomicrographs were taken under phase-contrast microscope.

Wound Healing Assay

Sub-confluent cultures of cells in 6-well plates were wounded using pipette tips, as previously reported (Zhang *et al.*, 2010), treated with or without drugs and allowed to migrate into the denuded area over a 24-h period. The migration of cells was visualized at a 10X magnification using an Axiovert 200 Inverted Fluorescence Microscope (Zeiss, Göttingen, Germany), with pictures taken using a mounted Canon Powershot A640 digital camera (Canon USA, Lake Success, NY). Cells that migrated into the denuded area were quantified.

Cell Migration Assays

Cell migration experiments were carried out and quantified as previously reported (Siddiquee *et al.*, 2007a; Siddiquee *et al.*, 2007b) and using Bio-Coat migration chambers (BD Biosciences, Bedford, MA) of 24-well companion plates with cell culture inserts containing 8 μm pore size filters, according to the manufacturer's protocol.

Substrate Embedded Gelatin Zymography Assay

Conditioned medium was collected from cells (5×10^5 per well in 6-well plate) cultured in 0.5% serum-containing medium for 48 h and samples subjected to native SDS-PAGE, as previously reported (Matsuo *et al.*, 2007), with some modifications. Briefly, non-denatured, non-reduced culture fluid samples were separated under non-reducing conditions on 10% SDS-PAGE gel containing 0.1% gelatin. After electrophoresis, the gel was incubated with 2.5% Triton X-100 at room temperature for 2 h and then incubated in gelatinase buffer (50 mM Tris-HCl, pH 7.5, 50 mM NaCl, and 10 mM $CaCl_2$) at 37°C with gentle shaking for 12–24 h. Thereafter, the gel was stained with 0.25% Coomassie brilliant blue R-250 for 4–6 h and destained until the appearance of clear bands. Areas showing enzyme activity showed up as regions of negative staining.

Hematoxylin and Eosin staining

Fresh tumor tissues from mice were embedded in OCT compound, frozen rapidly on dry ice, and the blocks were stored at −80°C. The frozen tissues were cryosectioned to 14 μm at −20°C and allowed to dry at 37°C for 30 min. The slides were fixed in cold acetone for 10 min, air-dried for 30 min, washed 2X in deionized water, and then stained for 5 min in Hematoxylin. After washing in distilled water for 1 min, slides were submerged in methanol with 1% HCl, and dipped in water with 0.1% $NH_4(OH)_2$. The tissues were then stained in acidified eosin for 1–2 min, followed by dehydration with 95% and 100% ethanol for 2 min, changing two times. Slides were allowed to air-dry, then submerged 3X in xylene for 3 min each and mounted. The tissues were observed and photos were taken under light microscopy.

Mice and in vivo tumor studies

Six-week-old female athymic nude mice were purchased from Harlan (Indianapolis, IN) and maintained in the institutional animal facilities approved by the American Association for Accreditation of Laboratory Animal Care. Athymic nude mice were injected intraperitoneally with 5×10^6 cells in 200 μL of PBS. Animals were evaluated twice per week for tumor growth or abdominal swelling. Ten days after tumor cell inoculation, mice were treated with DMSO (50%, 100 μL), cisplatin, cisplatin + ZD1839 (50 mg/kg), or cisplatin + S3I-201 (3 mg/kg) every 2 or 3 days. Approximately 25–39 days after the inoculation and on the development of visible abdominal swelling, the animals were euthanized. The peritoneal and thoracic cavities were exposed, tumor location and sizes were noted and tumor nodules were photographed, and counted for graphical representation.

Ovarian cancer patients' tumor tissues

To confirm the results from the cell line studies, analysis of EGFR, Stat3, E-cadherin, Vimentin, and Snail expression and/or activities was performed on tumor tissues from ovarian cancer patients. Specifically, when patients were diagnosed with a pelvic mass suspected to be ovarian cancer, Florida Hospital's Institutional Review Board (IRB)-approved informed consent was obtained. At the time of cytoreductive surgery the mass was confirmed by the Pathology Department to be ovarian cancer at which time the tumor sample was weighed and snap frozen in liquid nitrogen. The tissue specimens were ground in liquid nitrogen using a mortar and pestle and immediately subjected to lysate preparation following the protocol for whole-cell lysate preparation. Drug resistance/sensitivity tests results were obtained through Oncotech or Precision Therapeutics, which offers an *ex vivo* assay designed to predict the sensitivity and resistance of a given patient's solid tumor to a variety of chemotherapy agents. Clinical resistance is defined as relapse within 6 months and sensitive is relapse after 12 months off therapy.

Statistical Analysis

Statistical analysis was performed on mean values using Prism GraphPad Software, Inc. (La Jolla, CA). The significance of differences between groups was determined by paired *t*-test at $p < 0.05^*$, $<0.01^{**}$, and $< 0.001^{***}$.

Supplementary Material

Refer to Web version on PubMed Central for supplementary material.

Acknowledgments

Abbreviations

|	
STAT	signal transducer and activator of transcription
EGFR	epidermal growth factor receptor
MAPK	mitogen-activated protein kinase
MEK	MAP kinase kinase
EMT	epithelial-mesenchymal transition
Jak	Janus kinase
VEGF	vascular endothelial growth factor
PD	PD98059
S3I	S3I-201
ZD	ZD1839 (Iressa)

References

Ahmed N, Thompson EW, Quinn MA. Epithelial-mesenchymal interconversions in normal ovarian surface epithelium and ovarian carcinomas: an exception to the norm. J Cell Physiol. 2007; 213:581–588. [PubMed: 17708542]

Aoki Y, Feldman GM, Tosato G. Inhibition of STAT3 signaling induces apoptosis and decreases survivin expression in primary effusion lymphoma. Blood. 2003; 101:1535–42. Epub 2002 Oct 3. [PubMed: 12393476]

Arany I, Megyesi JK, Kaneto H, Price PM, Safirstein RL. Cisplatin-induced cell death is EGFR/src/ERK signaling dependent in mouse proximal tubule cells. Am J Physiol Renal Physiol. 2004; 287:F543–9. [PubMed: 15149969]

Arumugam T, Ramachandran V, Fournier KF, Wang H, Marquis L, Abbruzzese JL, et al. Epithelial to mesenchymal transition contributes to drug resistance in pancreatic cancer. Cancer Res. 2009; 69:5820–8. [PubMed: 19584296]

Avizienyte E, Frame MC. Src and FAK signalling controls adhesion fate and the epithelial-to-mesenchymal transition. Curr Opin Cell Biol. 2005; 17:542–547. [PubMed: 16099634]

Bhattacharya S, Ray RM, Johnson LR. STAT3-mediated transcription of Bcl-2, Mcl-1 and c-IAP2 prevents apoptosis in polyamine-depleted cells. Biochem J. 2005; 392:335–44. [PubMed: 16048438]

Blume-Jensen P, Hunter T. Oncogenic kinase signalling. Nature. 2001; 411:355–65. [PubMed: 11357143]

Bowden ET, Barth M, Thomas D, Glazer RI, Mueller SC. An invasion-related complex of cortactin, paxillin and PKCm associates with invadopodia at sites of extracellular matrix degradation. Oncogene. 1999; 18:4440–4449. [PubMed: 10442635]

Bowman T, Garcia R, Turkson J, Jove R. STATs in oncogenesis. Oncogene. 2000; 19:2474–2488. [PubMed: 10851046]

Brabec V, Kasparkova J. Modifications of DNA by platinum complexes. Relation to resistance of tumors to platinum antitumor drugs. Drug Resist Updat. 2005; 8:131–46. [PubMed: 15894512]

Bromberg JF, Wrzeszczynska MH, Devgan G, Zhao Y, Pestell RG, Albanese C, et al. Stat3 as an Oncogene. Cell. 1999; 98:295–303. [PubMed: 10458605]

Burke WM, Jin X, Lin HJ, Huang M, Liu R, Reynolds RK, et al. Inhibition of constitutively active Stat3 suppresses growth of human ovarian and breast cancer cells. Oncogene. 2001; 20:7925–7934. [PubMed: 11753675]

Catlett-Falcone R, Landowski TH, Oshiro MM, Turkson J, Levitzki A, Savino R, et al. Constitutive activation of Stat3 signaling confers resistance to apoptosis in human U266 myeloma cells. Immunity. 1999; 10:105–115. [PubMed: 10023775]

Chan JK, Pham H, You XJ, Cloven NG, Burger RA, Rose GS, et al. Suppression of ovarian cancer cell tumorigenicity and evasion of Cisplatin resistance using a truncated epidermal growth factor receptor in a rat model. Cancer Res. 2005; 65:3243–8. [PubMed: 15833856]

Cui W, Yazlovitskaya EM, Mayo MS, Pelling JC, Persons DL. Cisplatin-induced response of c-jun N-terminal kinase 1 and extracellular signal--regulated protein kinases 1 and 2 in a series of cisplatin-resistant ovarian carcinoma cell lines. Mol Carcinog. 2000; 29:219–28. [PubMed: 11170260]

Dancey JE, Freidlin B. Targeting epidermal growth factor receptor--are we missing the mark? Lancet. 2003; 362:62–4. [PubMed: 12853203]

Darnell JE. Validating Stat3 in cancer therapy. Nat Med. 2005; 11:595–6. [PubMed: 15937466]

Desai B, Ma T, Chellaiah MA. Invadopodia and matrix degradation, a new property of prostate cancer cells during migration and invasion. J Biol Chem. 2008; 283:13856–66. [PubMed: 18337256]

Duan Z, Foster R, Bell DA, Mahoney J, Wolak K, Vaidya A, et al. Signal Transducers and Activators of Transcription 3 Pathway Activation in Drug-Resistant Ovarian Cancer. Cancer Res. 2006; 12:5056–5063.

Epling-Burnette PK, Lui JH, Catlette-Falcone R, Turkson J, Oshiro M, Kothapalli R, et al. Inhibition of STAT3 signaling leads to apoptosis of leukemic large granular lymphocytes and decreased Mcl-1 expression. J Clin Invest. 2001; 107:351–362. [PubMed: 11160159]

Fajac A, Da Silva J, Ahomadegbe JC, Rateau JG, Bernaudin JF, GR, et al. Cisplatin-induced apoptosis and p53 gene status in a cisplatin-resistant human ovarian carcinoma cell line. Int J Cancer. 1996; 68:67–74. [PubMed: 8895543]

Gallagher WM, Cairney M, Schott B, Roninson IB, Brown R. Identification of p53 genetic suppressor elements which confer resistance to cisplatin. Oncogene. 1997; 14:185–93. [PubMed: 9010220]

Gan Y, Shi C, Inge L, Hibner M, Balducci J, Huang Y. Differential roles of ERK and Akt pathways in regulation of EGFR-mediated signaling and motility in prostate cancer cells. Oncogene. 2010; 29:4947–58. [PubMed: 20562913]

Gonzalez VM, Fuertes MA, Alonso C, Perez JM. Is cisplatin-induced cell death always produced by apoptosis? Mol Pharmacol. 2001; 59:657–63. [PubMed: 11259608]

Gritsko T, Williams A, Turkson J, Kaneko S, Bowman T, Huang M, et al. Persistent activation of stat3 signaling induces survivin gene expression and confers resistance to apoptosis in human breast cancer cells. Clin Cancer Res. 2006; 12:11–9. [PubMed: 16397018]

Huang M, Page C, Reynolds RK, Lin J. Constitutive activation of stat 3 oncogene product in human ovarian carcinoma cells. Gynecol Oncol. 2000; 79:67–73. [PubMed: 11006034]

Ikuta K, Takemura K, Kihara M, Naito S, Lee E, Shimizu E, et al. Defects in apoptotic signal transduction in cisplatin-resistant non-small cell lung cancer cells. Oncol Rep. 2005; 13:1229–34. [PubMed: 15870947]

Kassouf W, Dinney CP, Brown G, McConkey DJ, Diehl AJ, Bar-Eli M, et al. Uncoupling between epidermal growth factor receptor and downstream signals defines resistance to the antiproliferative effect of Gefitinib in bladder cancer cells. Cancer Res. 2005; 65:10524–35. [PubMed: 16288045]

Kelland LR, Sharp SY, O'Neill CF, Raynaud FI, Beale PJ, Judson IR. Mini-review: discovery and development of platinum complexes designed to circumvent cisplatin resistance. J Inorg Biochem. 1999; 77:111–5. [PubMed: 10626362]

Kim YK, Kim HJ, Kwon CH, Kim JH, Woo JS, Jung JS, et al. Role of ERK activation in cisplatin-induced apoptosis in OK renal epithelial cells. J Appl Toxicol. 2005; 25:374–82. [PubMed: 16013042]

Lee MY, Chou CY, Tang MJ, Shen MR. Epithelial-mesenchymal transition in cervical cancer: correlation with tumor progression, epidermal growth factor receptor overexpression, and snail up-regulation. Clin Cancer Res. 2008; 14:4743–50. [PubMed: 18676743]

Matsuo M, Sakurai H, Koizumi K, Saiki I. Curcumin inhibits the formation of capillary-like tubes by rat lymphatic endothelial cells. Cancer Lett. 2007; 251:288–95. [PubMed: 17197075]

Niu G, Wright KL, Huang M, Song L, Haura E, Turkson J, et al. Constitutive Stat3 activity up-regulates VEGF expression and tumor angiogenesis. Oncogene. 2002; 21:2000–2008. [PubMed: 11960372]

Richardson A, Kaye SB. Drug resistance in ovarian cancer: the emerging importance of gene transcription and spatio-temporal regulation of resistance. Drug Resist Updat. 2005; 8:311–21. [PubMed: 16233989]

Selvendiran K, Bratasz A, Kuppusamy ML, Tazi MF, Rivera BK, Kuppusamy P. Hypoxia induces chemoresistance in ovarian cancer cells by activation of signal transducer and activator of transcription 3. Int J Cancer. 2009; 125:2198–204. [PubMed: 19623660]

Selvendiran K, Bratasz A, Tong L, Ignarro LJ, Kuppusamy P. NCX-4016, a nitro-derivative of aspirin, inhibits EGFR and STAT3 signaling and modulates Bcl-2 proteins in cisplatin-resistant human ovarian cancer cells and xenografts. Cell Cycle. 2008; 7:81–8. [PubMed: 18196976]

Shao H, Cheng HY, Cook RG, Tweardy DJ. Identification and characterization of signal transducer and activator of transcription 3 recruitment sites within the epidermal growth factor receptor. Cancer Res. 2003; 63:3923–30. [PubMed: 12873986]

Siddiquee K, Glenn M, Gunning P, Katt WP, Zhang S, Schroeck C, et al. An oxazole-based small-molecule Stat3 inhibitor modulates Stat3 stability and processing and induces antitumor cell effects. ACS Chem Biol. 2007a; 2:787–98. [PubMed: 18154266]

Siddiquee K, Zhang S, Guida WC, Blaskovich MA, Greedy B, Lawrence H, et al. Selective chemical probe inhibitor of Stat3, identified through structure-based virtual screening, induces antitumor activity. Proc Natl Acad Sci U S A. 2007b; 104:7391–6. [PubMed: 17463090]

Song H, Sondak VK, Barber DL, Reid TJJL. Modulation of Janus kinase 2 by cisplatin in cancer cells. Int J Oncol. 2004; 24:1017–26. [PubMed: 15010843]

Thiery JP. Epithelial-mesenchymal transitions in tumour progression. Nat Rev Cancer. 2002; 2:442–454. [PubMed: 12189386]

Tice DA, Biscardi JS, Nickles AL, Parsons SJ. Mechanism of biological synergy between cellular Src and epidermal growth factor receptor. Proc Natl Acad Sci U S A. 1999; 96:1415–1420. [PubMed: 9990038]

Turkson J. STAT proteins as novel targets for cancer drug discovery. Expert Opin Ther Targets. 2004; 8:409–422. [PubMed: 15469392]

Turkson J, Bowman T, Garcia R, Caldenhoven E, De Groot RP, Jove R. Stat3 activation by Src induces specific gene regulation and is required for cell transformation. Mol Cell Biol. 1998; 18:2545–2552. [PubMed: 9566874]

Villedieu M, Deslandes E, Duval M, Heron JF, Gauduchon P, Poulain L. Acquisition of chemoresistance following discontinuous exposures to cisplatin is associated in ovarian carcinoma cells with progressive alteration of FAK, ERK and p38 activation in response to treatment. Gynecol Oncol. 2006; 101:507–19. [PubMed: 16387351]

Wang G, Reed E, Li QQ. Molecular basis of cellular response to cisplatin chemotherapy in non-small cell lung cancer (Review). Oncol Rep. 2004; 12:955–65. [PubMed: 15492778]

Yu H, Jove R. The STATS of Cancer-New molecular targets come of age. Nat Rev Cancer. 2004; 4:97–105. [PubMed: 14964307]

Zhang X, Yue P, Fletcher S, Zhao W, Gunning PT, Turkson J. A novel small-molecule disrupts Stat3 SH2 domain-phosphotyrosine interactions and Stat3-dependent tumor processes. Biochem Pharmacol. 2010; 79:1398–409. [PubMed: 20067773]

Zhang Y, Turkson J, Carter-Su C, Smithgall T, Levitzki A, Kraker A, et al. Activation of Stat3 in v-Src Transformed Fibroblasts Requires Cooperation of Jak1 Kinase Activity. J Biol Chem. 2000; 275:24935–24944. [PubMed: 10823829]
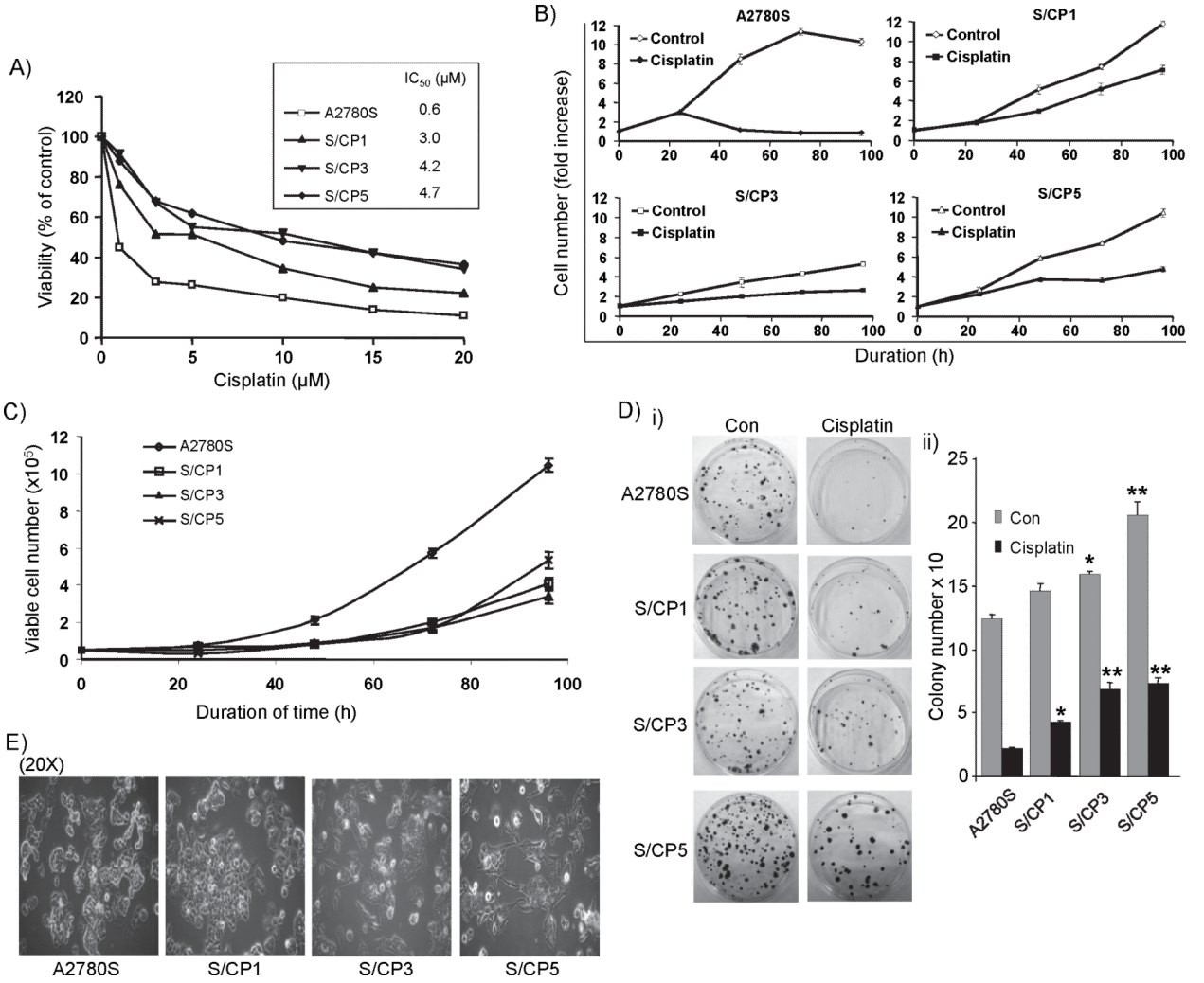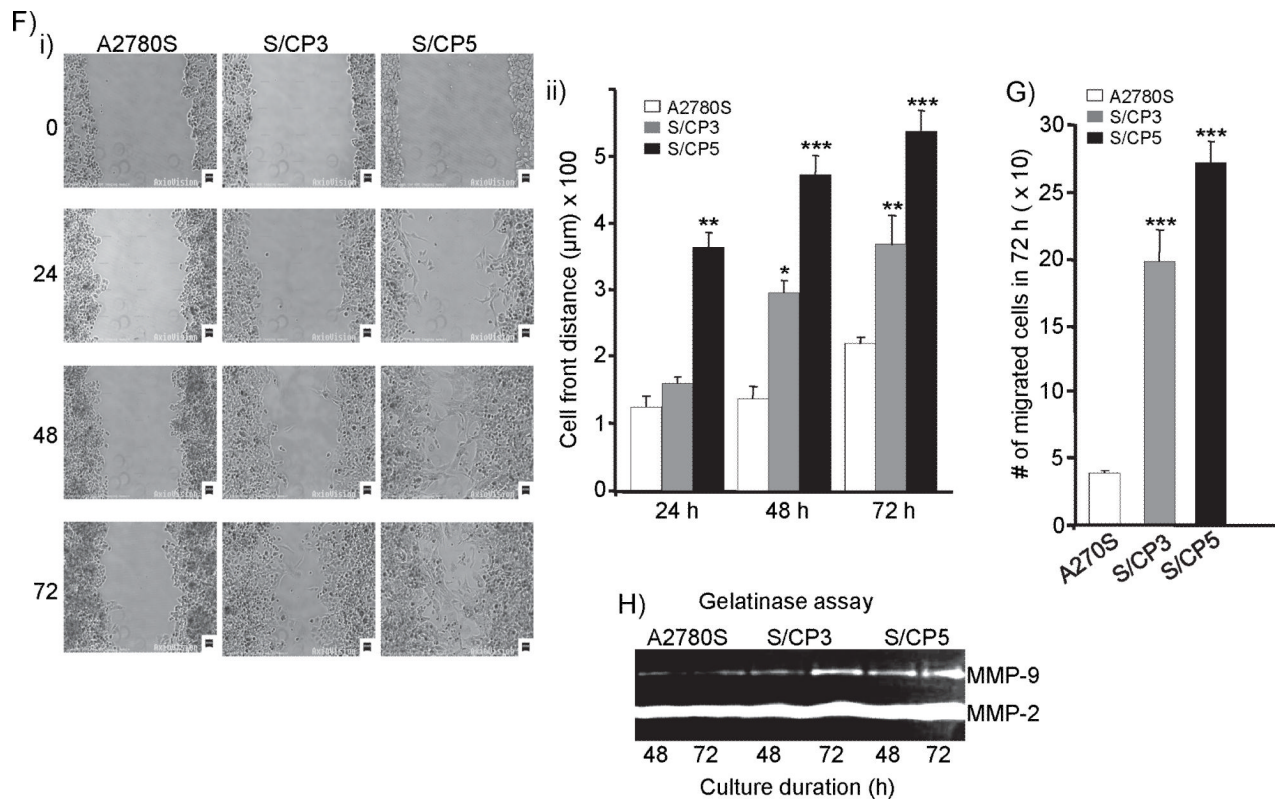
Figure 1. Growth, viability, survival, migration, gelatinase activity, and morphology properties of Cisplatin-resistant cells
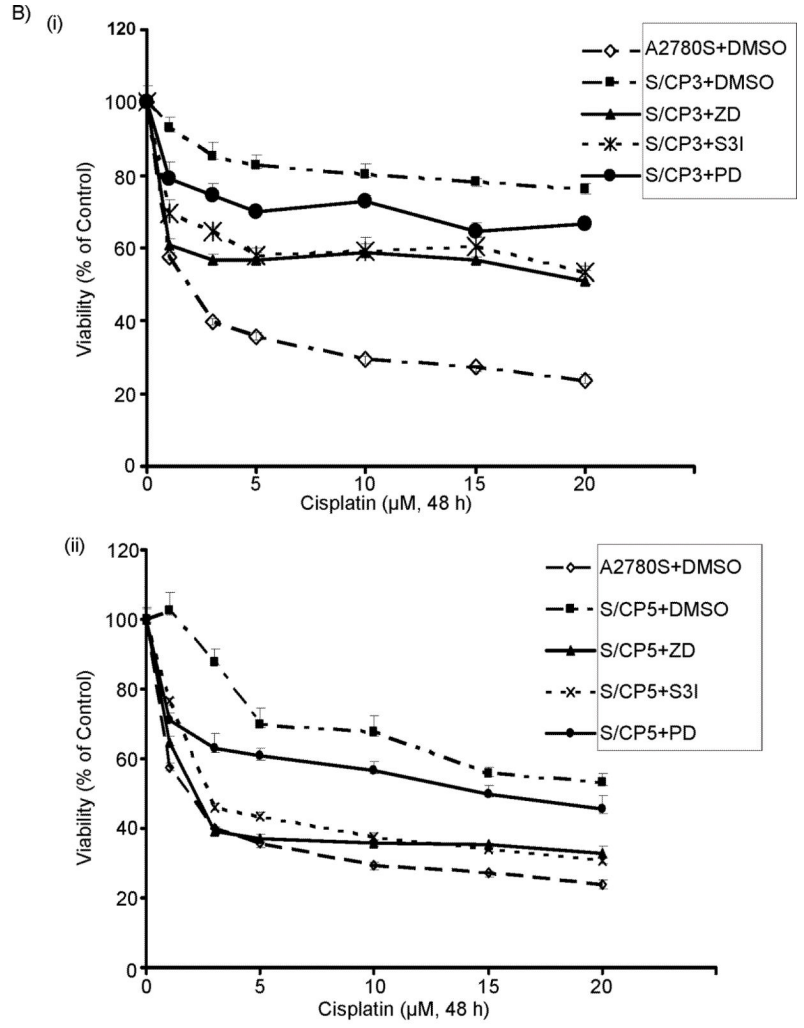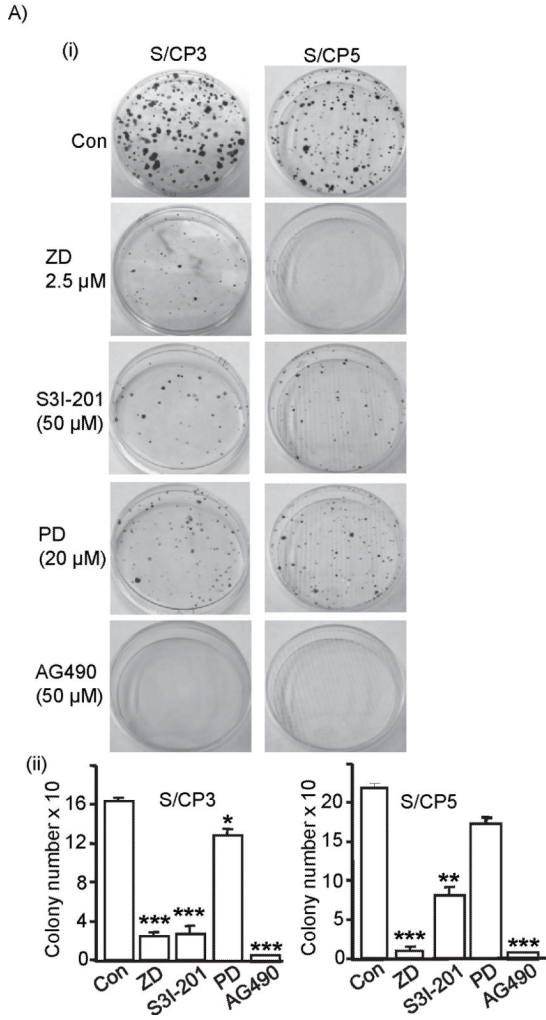
(A and B) Cyquant cell viability assay of cisplatin-sensitive, A2780S and the cisplatin-resistant S/CP1, S/CP3 and S/CP5 cells in culture and (A) treated with increasing concentration of cisplatin for 48 h and plotted as viability against cisplatin concentration, IC_{50} values (insert panel) were derived from the respective graphical representations, or (B) untreated (control) or treated, respectively, with 1, 1, 3, and 5 μM cisplatin, for 0–96 h and viable cell numbers plotted against duration of treatment; (C) Cell growth curves for viable cell numbers assessed over 24–96 h by trypan blue exclusion/phase-contrast microscopy; (D) Colony survival assay for single-cell cultures of A2780S, S/CP1, S/CP3, and S/CP5 untreated (control, con) or treated once with 1, 1, 3, and 5 μM cisplatin, respectively, and allowed to culture until visible colonies were evident, which were stained with crystal violet and presented as photomicrographs (i) or enumerated and plotted as colony numbers (ii); (E) Phase-contrast microscopic examination of the morphology of A2780S, S/CP1, S/CP3 and S/CP5 cells in culture. Cultures were visualized at 20X magnification; (F) Cells in culture were wounded and allowed to migrate into the denuded area over 24–72 h. Cultures were visualized at 10X magnification by light microscopy and (i) presented as photomicrographs, or (ii) the distances traveled by the cell front into the denuded area were measured and plotted; G) Bio-Coat migration chamber assay and a plot of the number of migrated cells; and H) Zymography assay for gelatinolytic activity of the media from the cultures of A2780S, S/CP3 and S/CP5 cells cultured over 48 and 72 h. MMP-2 is represented by the band at 72 kDa, and its levels remain constant over 48–72 h. MMP-9 is represented by the band at 92 kDa, and its levels increase over the 48–72 h. Values are the mean and S.D. of 3–4 independent determinations, data are representative of 3–4 independent studies. p values, * - <0.05, ** - <0.01, and ***- <0.005.
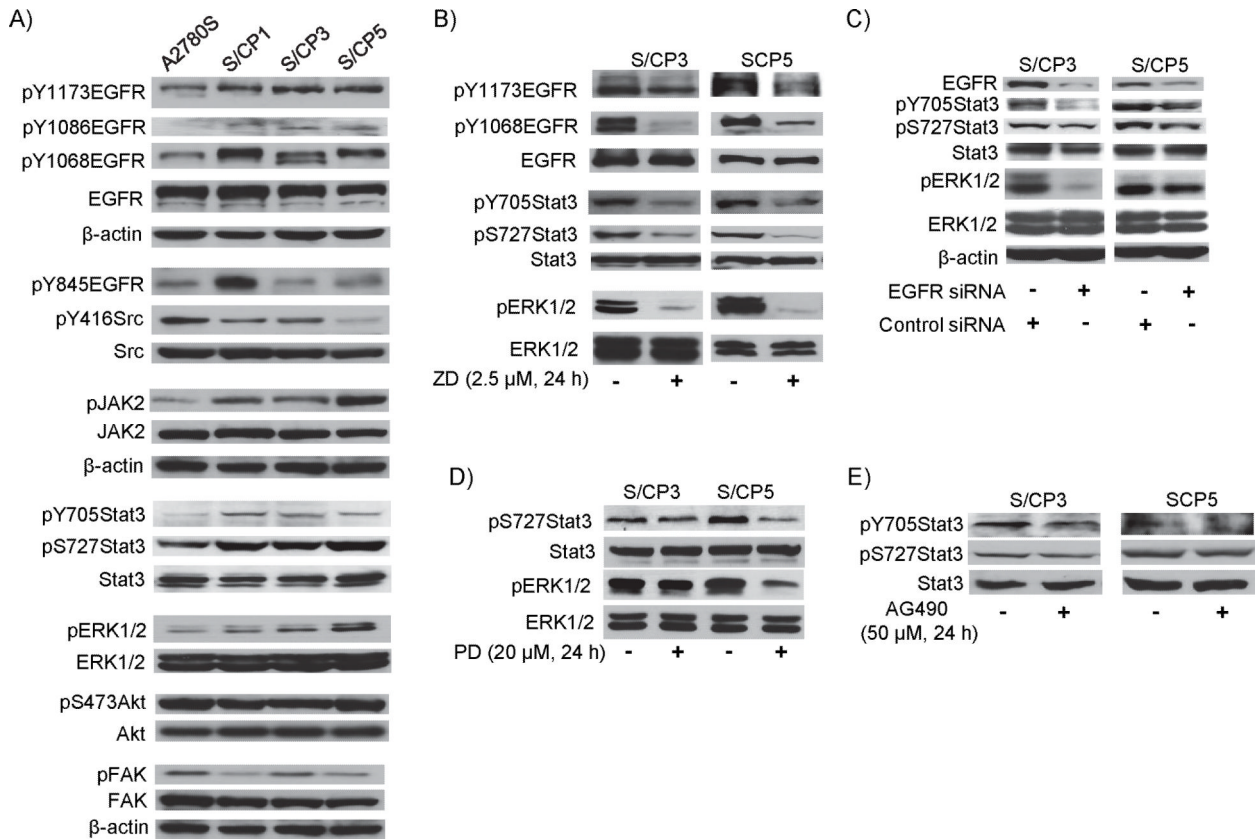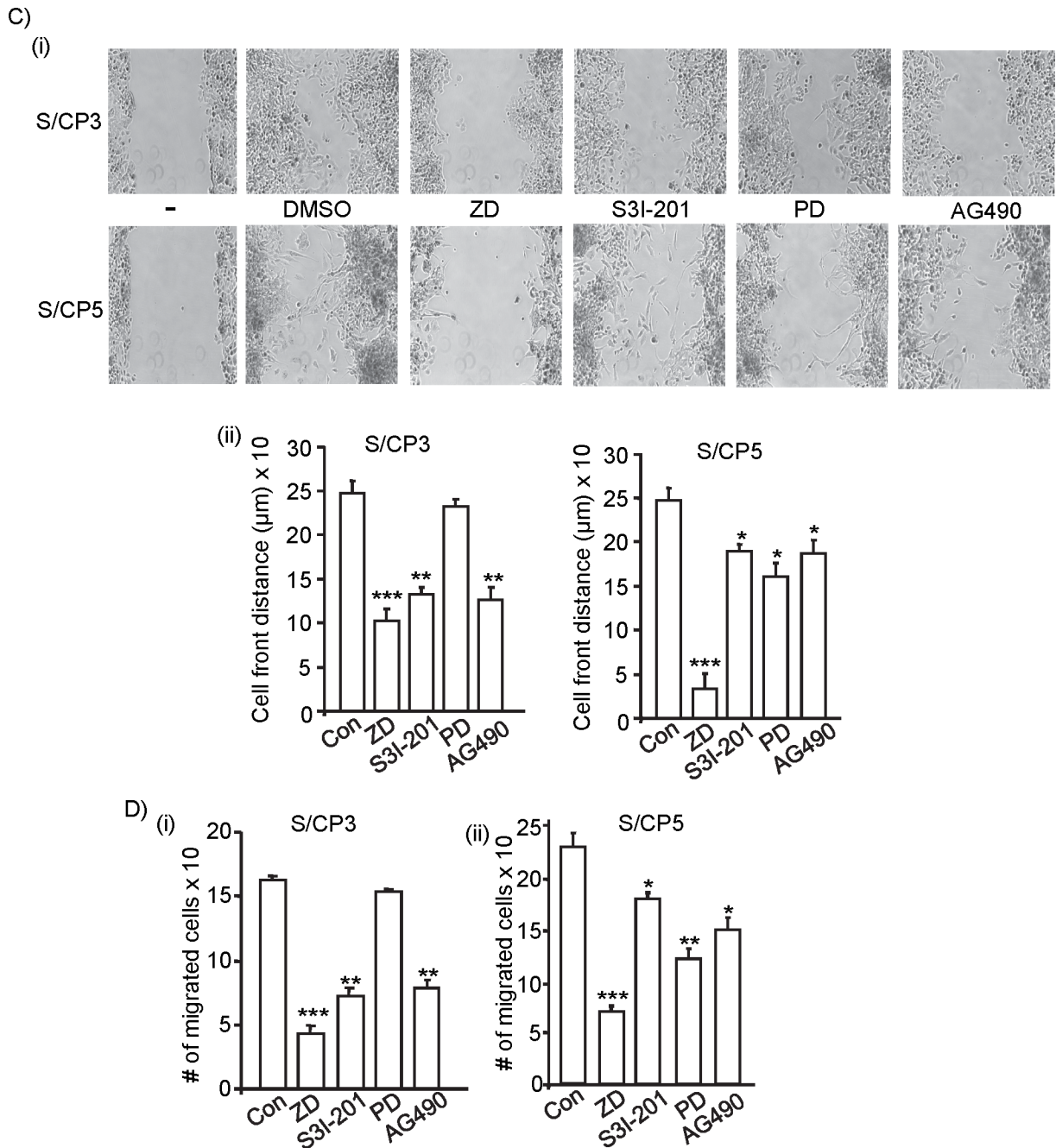
Figure 2. Immunoblotting analysis of the activation of EGFR, Stat3, Src, Jaks, Erk1/2, Akt, and focal adhesion kinase (FAK) and the effects of inhibitors

Immunoblotting analysis of whole-cell lysates from A2780S, S/CP1, S/CP3 or S/CP5 cells (A) untreated, or (B) treated with or without ZD 1839 (ZD), or (C) transfected with or without EGFR or control siRNA, or (D) treated with or without PD98059 (PD), or (E) treated with or without AG490 for the indicated times, and probing for pY1173EGFR, pY1086EGFR, pY1068EGFR, EGFR, pY845EGFR, pY416Src, Src, pJak2, Jak2, pY705Stat3, pS727Stat3, Stat3, pErk1/2, Erk1/2, pS473Akt, Akt, pFAK, or FAK and β-Actin. Positions of proteins in gel are labeled; control lanes (−) represent whole-cell lysates prepared from 0.05% DMSO-treated. Data are representative of 3–4 independent determinations.

A)

(i)

S/CP3   S/CP5

Con

ZD
2.5 µM

S3I-201
(50 µM)

PD
(20 µM)

AG490
(50 µM)

(ii)

B) (i)

(ii)

C)

(i)

S/CP3 | - | DMSO | ZD | S3I-201 | PD | AG490

S/CP5

(ii)

D) (i)

(ii)

Figure 3. Viability, Colony-survival, wound-healing, and Bio-Coat migration chamber assays of cells and the effects of cisplatin, inhibitors of EGFR, Stat3 and MEK-Erk

(A) S/CP3, S/CP5 cells in culture were untreated or treated once with Iressa (2.5 μM ZD), Stat3 inhibitor (50 μM S3I-201), MEK-Erk inhibitor (20 μM PD98059, PD), or the Jak inhibitor, AG490 (50 μM). Cells were allowed to culture until visible colonies were evident, which were stained and visualized under phase-contrast microscopy and (i) imaged or (ii) enumerated and plotted; (B) CyQuant assay for the effects on A2780S, S/CP3 and S/CP5 cell viability of treatments for 48 h with 0–20 μM cisplatin in the absence (DMSO) or presence of ZD (5 μM), S3I-201 (50 μM), or PD98059 (20 μM) and plotted as percent of control (DMSO-treated) cells; (C) Cells (S/CP3 and S/CP5) in culture were wounded and

untreated or treated once with ZD (2.5 µM), S3I-201 (50 µM), PD98059 (PD, 20 µM), or AG490 (50 µM) for 24 h and allowed to migrate into the denuded area. Cultures were visualized at 10X magnification by light microscopy and (i) presented as photomicrographs, or (ii) the measured distance traveled by the cell front into the denuded area is plotted; and (D) Plots of number of migrated cells in Bio-Coat migration chamber assay performed over 24 h and the effects of ZD (2.5 µM), S3I-201 (50 µM), and AG490 (50 µM). Values are the mean and S.D. of 3–4 independent determinations, data are representative of 3–4 independent studies. p values, * - <0.05, ** - <0.01, and ***- <0.005.
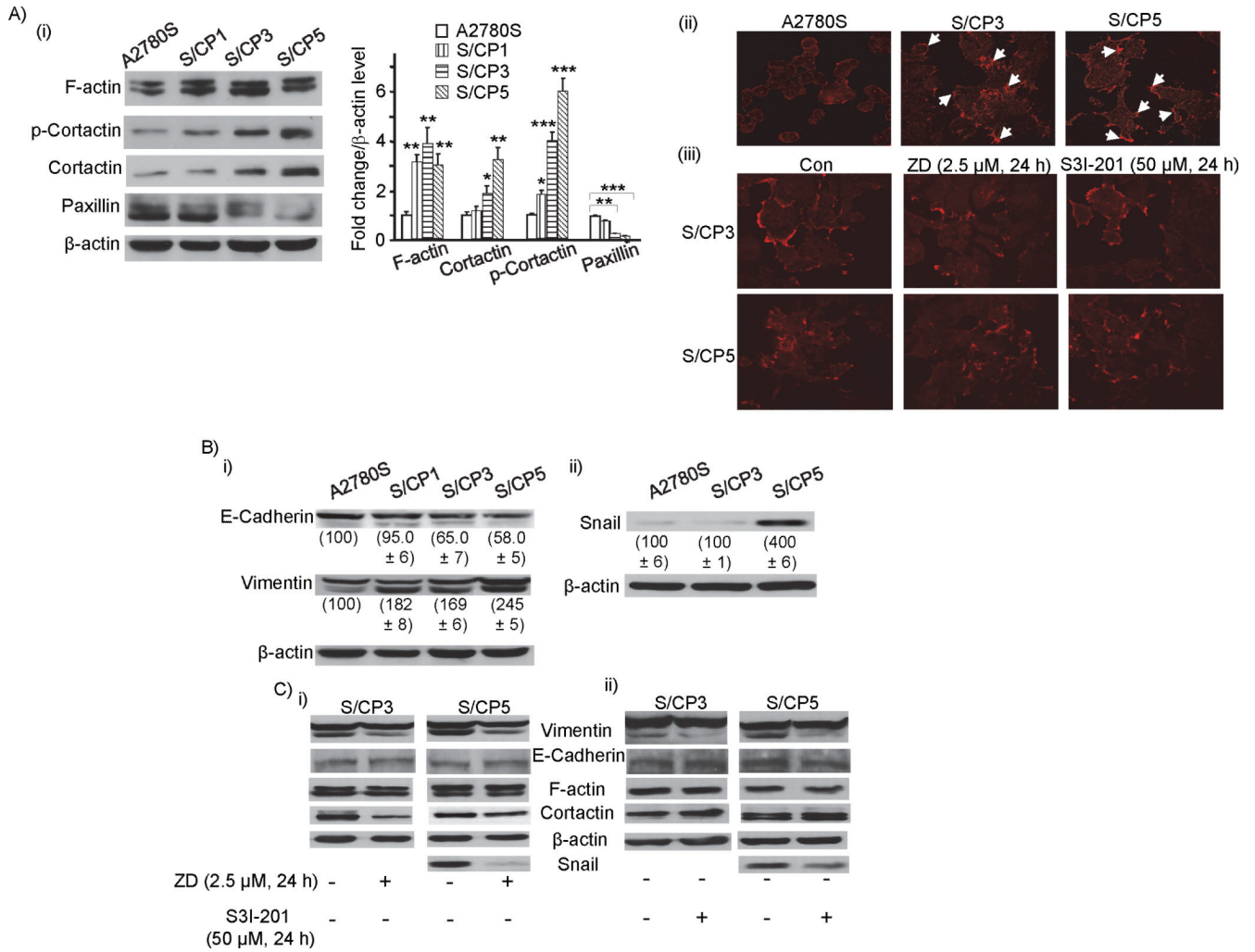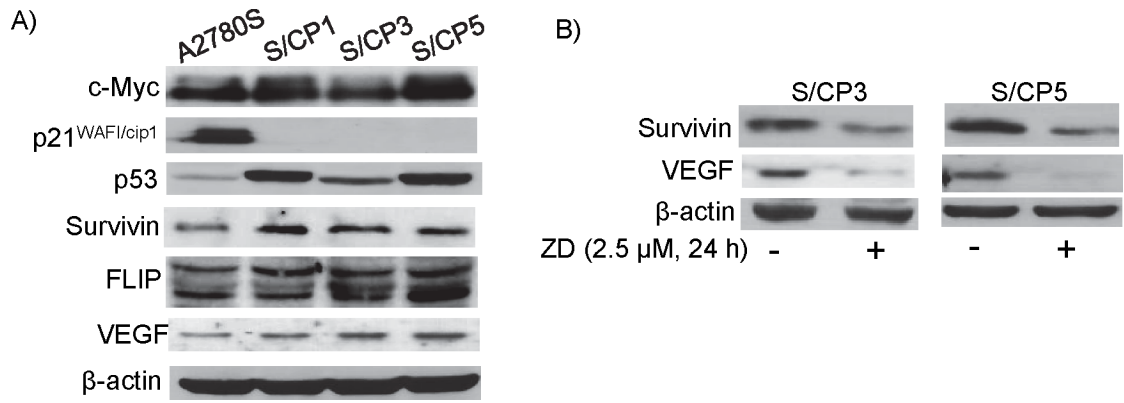
Figure 4. Immunoblotting analysis or fluorescence imaging of F-actin, Cortactin, Paxillin, E-Cadherin, Vimentin, and Snail and the effect of inhibitors of EGFR or Stat3

(A(i), B, and C) Immunoblotting analysis of whole-cell lysates from A2780S, S/CP1, S/CP3 or S/CP5 cells (A(i) and B) untreated or (C) treated with or without ZD1839 (ZD) (2.5 µM) or S3I-201 (50 µM) for the indicated times and probing for F-actin, Cortactin, Paxillin, E-Cadherin, Vimentin, Snail, and β-Actin; bands were quantified by ImageQuant and intensities relative to β-actin levels are plotted (A(i), right panel) or shown in parenthesis (B(i) and (ii)); or cells untreated (Aii) or treated (Aiii) with ZD (2.5 µM) or S3I-201 (50 µM) for 24 h were stained with anti-F-actin antibody (red) and analyzed by laser-scanning confocal microscopy for localization. Confocal images were collected using Leica TCS SP5 microscope. Positions of proteins in gel are labeled; control lanes (−) represent whole-cell lysates prepared from 0.05% DMSO-treated; White arrows show the localization of F-actin; Data are representative of 3–4 independent determinations; p values, * - <0.05, ** - <0.01, and ***- <0.005.
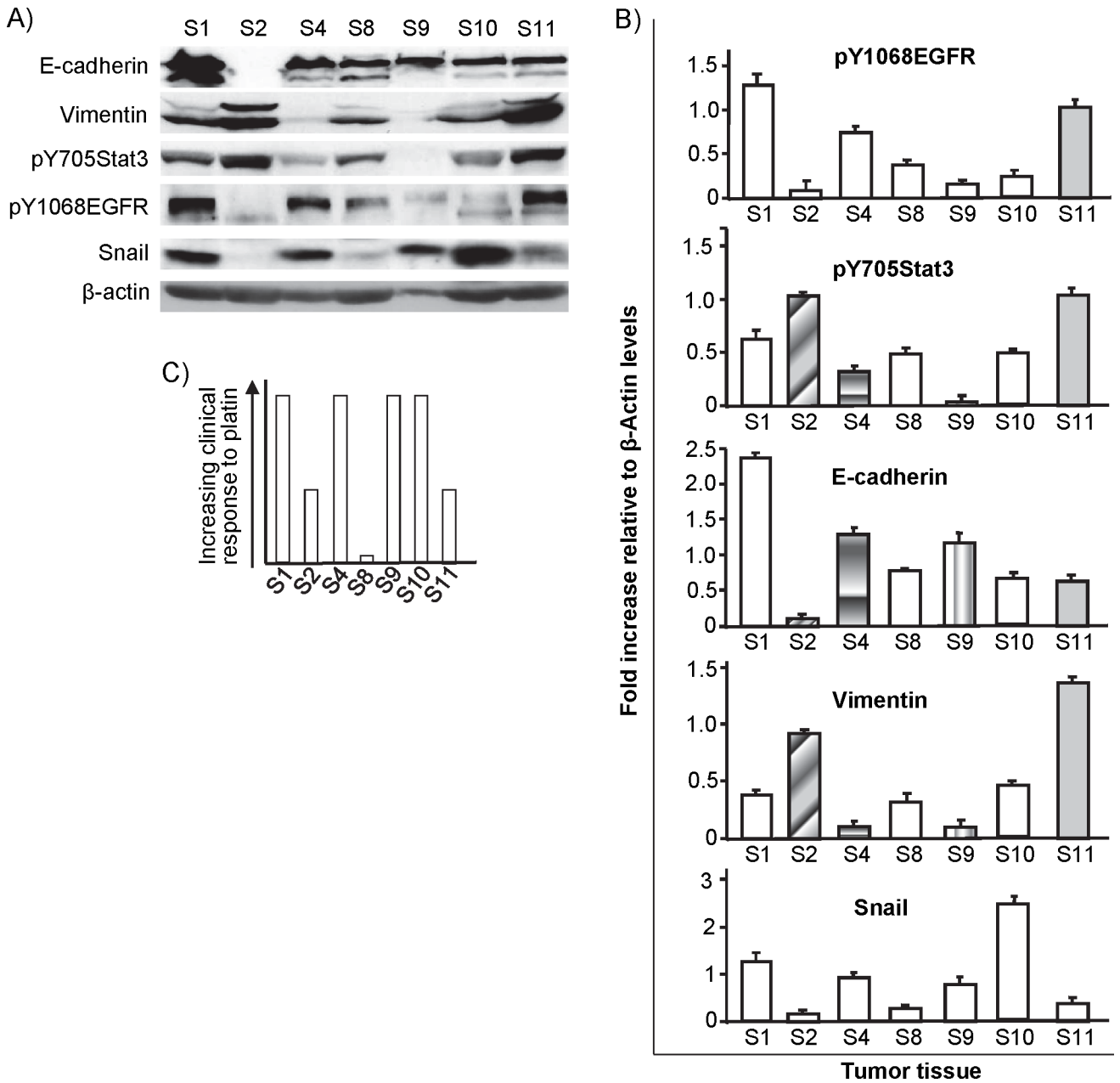
Figure 5. Analysis of pEGFR, pStat3, E-Cadherin, Vimentin, and Snail in human ovarian tumor tissues
Immunoblotting analysis of lysates from human ovarian cancer tissues, S1, S2, S4, S8, S9, S10, and S11 probing for (i) pY1068EGFR, pTyr705Stat3, E-Cadherin, Vimentin, and Snail; (ii) ImageQuant analysis of band intensity represented relative to β-Actin levels; and (C) Graphical representation of the clinical response to platin therapy for the designated tumors. Positions of proteins in gel are labeled; Data are representative of 2 independent determinations, values are the mean and S.D. of 2 independent determinations or acquired for individual patients.

A)

B)

Figure 6. Immunoblotting analysis of c-Myc, p21$^{WAF1/cip1}$, p53, Survivin, FLIP, and VEGF and the effects of EGFR inhibitor
Immunoblotting analysis of whole-cell lysates from A2780S, S/CP1, S/CP3 or S/CP5 cells (A) untreated or (B) treated with or without ZD1839 (ZD) (2.5 µM, 24 h) and probing for c-Myc, p21$^{WAF1/cip1}$, p53, Survivin, FLIP, and VEGF and β-Actin. Positions of proteins in gel are labeled; control lanes (−) represent whole-cell lysates prepared from 0.05% DMSO-treated. Data are representative of 3 independent determinations.
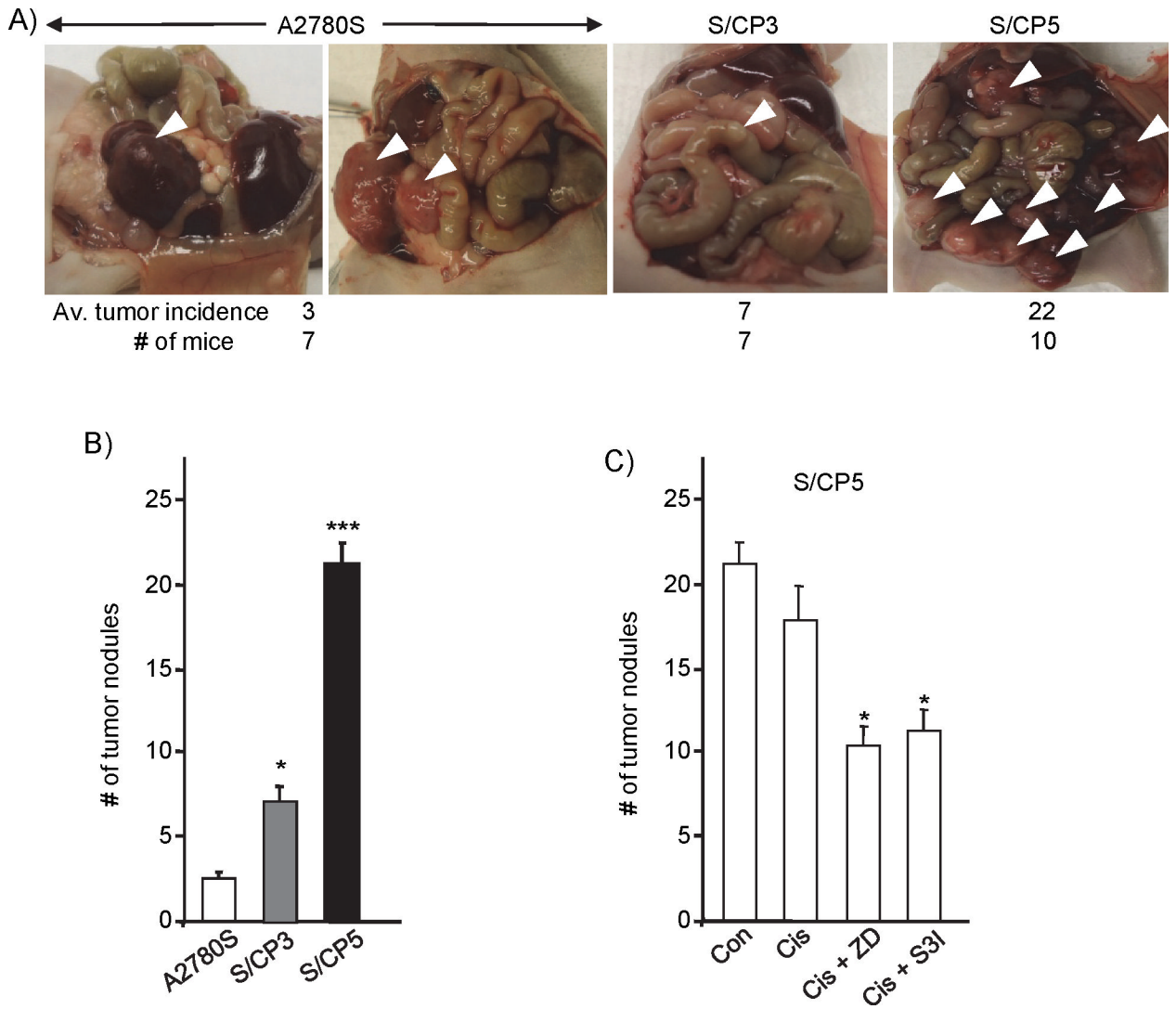
Figure 7. Intra-peritoneal (i.p.) human tumor xenografts of cisplatin-sensitive and resistant ovarian cancer lines and the antitumor effects of cisplatin alone and in combination with ZD1839, S3I-201 or PD98059

(A) Macroscopic images of i.p. models of human ovarian cancer lines, A2780S, S/CP3 and S/CP5; the numbers underneath represent tumor incidence and the number of mice in study; and (B and C) plots of number of tumor nodules developed in the intra-peritoneal area for the cisplatin-sensitive A2780S and the resistant S/CP3 and S/CP5 human ovarian cancer lines (B) and the effect of treatment with cisplatin alone and in combination with ZD1839, S3I-201, or PD98059 on the development of S/CP5 tumor nodules (C). Arrows indicate positions of tumors. Data are representative of 3 or 5 mice in each group; Values are the mean and S.D. from 7–10 tumor-bearing mice in each group. p values, * - <0.05, and *** - <0.005.
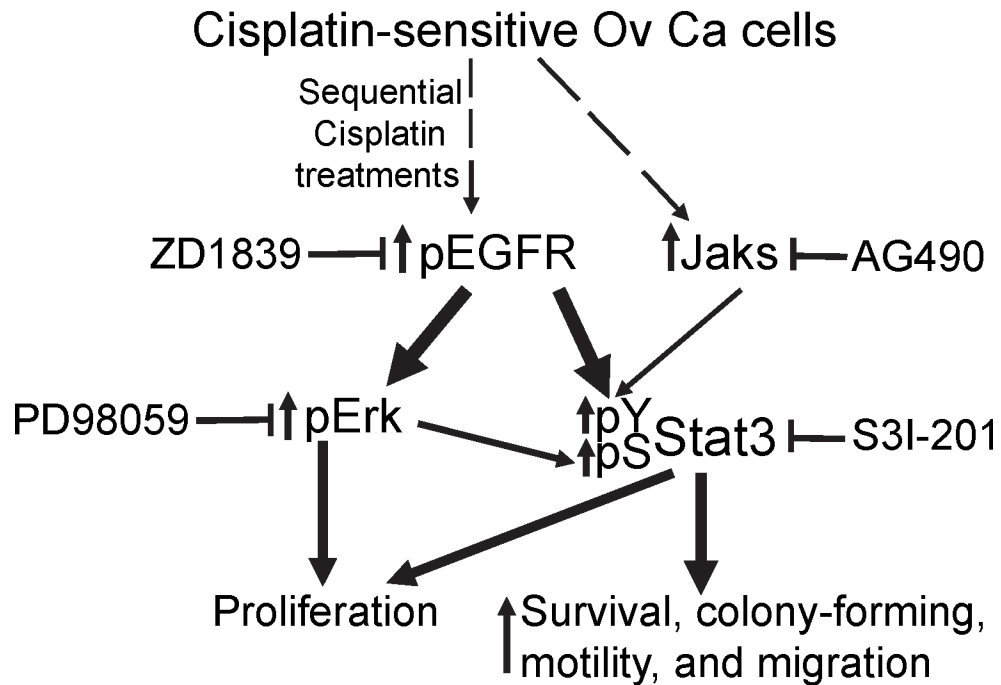
Figure 8. Model for hyperactivated tyrosine kinase-mediated Erk and Stat3 induction that promotes cisplatin-resistance in Ovarian Cancer (Ov Ca)

Sequential treatments with csplatin followed by recovery periods promote hyperactive EGFR, Jak tyrosine kinases and the events downstream. Specifically, hyperactive EGFR induces aberrant Erk1/2 activation, and EGFR kinase and to a lesser extent, Jak kinases promote constitutive tyrosine phosphorylation (pY) and activation of Stat3. Moreover, aberrant Erk1/2 activity induces the serine phosphorylation (pS) of Stat3. Both Erk1/2 and Stat3 activities transduce signals that support the proliferation of cisplatin-resistant ovarian cancer cells. Furthermore, EGFR signaling and Jak activation, largely through Stat3 activity support viability, and promote enhanced colony-forming ability, motility and the migration of the cisplatin resistant cells. The inhibition of EGFR by ZD1839 significantly represses pY705Stat3 and pS727Stat3 levels, and the inhibition of Jaks by AG490 moderately reduces pY05Stat3 levels, while the inhibition of Erk by PD98059 represses pS727Stat3 levels. The inhibition of Erk activity blocks cell proliferation, while the inhibition of EGFR, Stat3 or Jaks activity significantly diminishes proliferation, and blocks the colony-forming ability, motility and migration of cisplatin-resistant ovarian cancer cells. Broken lines indicate undetermined mechanisms of induction.